



## An acido- and photochromic molecular device that mimics triode action

Journal:	<i>ChemComm</i>
Manuscript ID	CC-COM-01-2016-000840.R1
Article Type:	Communication
Date Submitted by the Author:	26-Feb-2016
Complete List of Authors:	Remón, Patricia; Chalmers University of Technology, Department of Chemistry and Chemical Engineering Li, Shiming; Chalmers University of Technology, Department of Chemistry and Chemical Engineering Grotli, Morten; University of Gothenburg, Department of Chemistry and Molecular Biology Pischel, Uwe; University of Huelva, Department of Chemical Engineering, Physical Chemistry, and Organic Chemistry Andréasson, Joakim; Chalmers University of Technology, Department of Chemistry and Chemical Engineering

## COMMUNICATION

## An acido- and photochromic molecular device that mimics triode action†

Cite this: DOI: 10.1039/x0xx00000x

P. Remón,<sup>a</sup> S. M. Li,<sup>a</sup> M. Grøtli,<sup>b</sup> U. Pischel,<sup>\*c</sup> and J. Andréasson<sup>\*a</sup>

Received 00th January 2012,

Accepted 00th January 2012

DOI: 10.1039/x0xx00000x

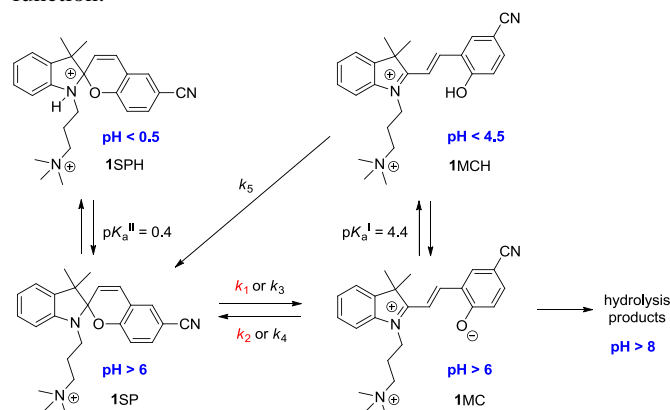
www.rsc.org/

**The photo-controlled shift of pH titration curves, describing the acidochromic behaviour of a spiropyran switch network, was harnessed for the realisation of a molecular triode. The intricate network can be correctly interpreted with respect to the pH dependence of the main involved species.**

The fascinating opportunities offered by light-controlled molecular switches are currently unfolding in research areas such as chemical biology, nanochemistry, materials science, and molecular information processing.<sup>1-9</sup> This preference is triggered by the possibility to change molecular and system's properties by light exposure in a reversible, waste-free, non-invasive, and spatiotemporally controlled fashion. With view on this, light has been increasingly used as stimuli to devise molecular devices capable of performing logic operations<sup>5, 10-14</sup> with different degrees of complexity, e.g., simple logic gates (AND, OR, NOR, *etc.*), elementary arithmetic operations (addition, subtraction), logic circuits (multiplexer, encoder, *etc.*), and memory devices.<sup>2, 15-22</sup>

In the semiconductor-driven world triodes/transistors play an archetypal role. Inspired by this, it is very appealing to devise molecules that are capable of mimicking the performance of these analogue electronic building blocks. Despite the conventional use of electrical signalling, chemical and photophysical phenomena can be interpreted along the lines of a molecular triode or transistor as well. One strategy is the exploitation of photochromic (dithienylethene) supramolecular systems for the all-photonic realization of photo-controlled emission modulation via energy transfer.<sup>23, 24</sup> A different approach was followed with a pH-sensitive fluorophore, whose electron-transfer-induced emission quenching can be additionally controlled by metal cation complexation. The

resulting  $pK_a$  shifts resemble the characteristics of triode *i-V* curves.<sup>25</sup> Finally, very recently the peculiar temperature-dependent operation of a fluorescent electrochemical switch was harnessed for demonstrating a transistor function.<sup>26</sup> Some of these systems require either intensive synthetic labour or a very specific chemical design. Others work with metal-cation inputs which may cause problems for the recycling of the function.



**Scheme 1.** Switch network of spiropyran **1**. The associated pH values are approximate and included for the purpose of orientation. The herein relevant rate constants of the thermally-induced processes (red) and photochromic processes (black) are colour-coded.

In an effort to base our chemical design on the generally and widely used class of photofunctional spiropyrans we came across a so far overlooked photo-controlled hysteresis effect in the pH titration curves describing the integrated acidochromic behaviour of such systems. Their application in bio-relevant contexts such as light-controlled DNA binding<sup>27-29</sup> and

interactions on proteins,<sup>30</sup> bioimaging,<sup>31-33</sup> or biosensing<sup>34</sup> provides additional incentive to explore their inherent functional character beyond the photochromic switching itself, for example for devising a molecular triode. This complements the conceptual importance of spiro-pyrans/-oxazines in molecular information processing as exemplified by molecular memories and Fuzzy logics.<sup>35-39</sup>

Spiropyrans, such as the water-soluble **1**, are implied in photo- and acidochromic switching between three states: spiro form (SP), merocyanine (MC), and protonated merocyanine (MCH); Scheme 1.<sup>40</sup> In very acidic solution (pH < 0.5) the protonated spiro form SPH is abundant, while the undesired hydrolysis of the MC form intervenes especially at basic pH (pH > 8).<sup>40, 41</sup> Therefore we limited our study to an intermediate pH window between 1.5 and 8.

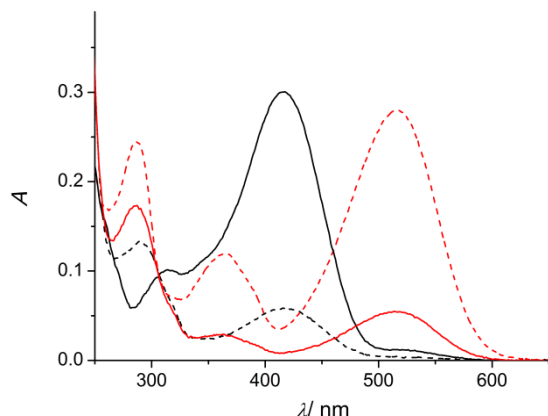


**Figure 1.** UV/vis absorption spectra of **1** (20  $\mu\text{M}$  in water) for the thermal equilibrium (pH 3, black full line; pH 6, red full line) and in the PSS (pH 3, black dashed line; pH 6, red dashed line).

In aqueous solution at pH  $\geq 6$  **1SP** is in a thermal ("dark") equilibrium with **1MC** ( $K = k_1/k_2 = 0.16$  at pH 7) which can be displaced by protonation of the merocyanine to yield the thermally stable **1MCH** ( $\text{p}K_a^1 = 4.4$ ).<sup>40</sup> Hence, at high pH (pH  $\geq 6$ ) the SP form is dominant, whereas at low pH (pH  $\leq 4.5$ ) the MCH form prevails. This is clearly manifested in the corresponding UV/vis absorption spectra (see Figure 1). The small **1MC** absorption band ( $\lambda_{\text{max}} = 515$  nm) at pH 6 is contrasted by the dominating **1MCH** absorption band ( $\lambda_{\text{max}} = 416$  nm) at pH 3.

The situation changes dramatically when UV light ( $\lambda = 254$  nm, power density of  $700 \mu\text{W cm}^{-2}$ ) is applied until reaching the photostationary state (PSS). Now **1SP** is photoisomerised to **1MC** at pH  $\geq 6$ . The quantum yields ( $\Phi$ ) of the ring-opening and closing paths are 0.040 and 0.012, respectively.<sup>‡40</sup> However, at pH  $\leq 4.5$  UV exposure culminates in the enrichment of the sample in **1SP**; see Figure 1. This is reasoned with the highly competitive ring closure of the **1MCH** form to **1SP** ( $\Phi = 0.21$ ).

The photo-driven variation of the composition of the switch network has consequences for the titration curve monitoring the normalised concentration of the merocyanine form ( $[\text{1MC}]/[\text{1MC}]_{\text{max}}$ ) in dependence on the pH; see Figure 2.

**1MC** can be conveniently followed by its absorbance at  $\lambda = 515$  nm, where none of the other forms of **1** absorb at any pH. In the absence of light irradiation, the concentration of **1MC** is mainly determined by the degree of protonation producing **1MCH**. However, as described above, **1MCH** is efficiently photo-converted to **1SP** and thereby removed from the protonation equilibrium involving **1MC**. Consequently, the re-establishment of the thus disturbed equilibrium leads to a decreased relative **1MC** concentration as compared to the same pH in the absence of UV irradiation. This is experimentally expressed in a positive shift of the "apparent  $\text{p}K_a$ " value by about 1.6 units. Note that this shift is the result of the integrated behaviour of the switch network and conceptually different from the observation of  $\text{p}K_a$  shifts on photo-conversion between two isomers with differing basicity.<sup>42, 43</sup>

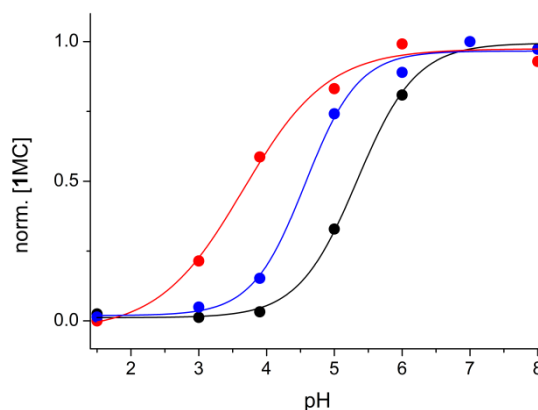


**Figure 2.** pH titration curves monitoring the normalised **1MC** concentration ( $[\text{1MC}]/[\text{1MC}]_{\text{max}}$ ). The experimental data points were obtained for fully equilibrated systems (i.e., thermal equilibrium and/or PSS). Colour codes: red = absence of irradiation (dark reaction); black = irradiation with 254-nm light; blue = irradiation with 254-nm light with an attenuated UV intensity (to 1.3%). The lines correspond to sigmoid fits for guiding the eye.

Furthermore it was foreseen that the UV irradiation with an attenuated UV intensity would reveal an intermediate situation, signalled by a pH titration curve situated between the two beforehand discussed cases (thermal processes and irradiation at full UV intensity). Gratifyingly this was indeed verified for an attenuation to 1.3% of full UV intensity; see Figure 2.

The working principle and characteristics of a triode can be described as follows. Upon heating of the cathode by a filament a thermoionic emission of electrons results, which is collected by a positively charged anode plate. On their way the electrons have to pass a grid which acts like a gate. The anode current-voltage ( $i_A$ - $V_A$ ) curve can be shifted by the variation of the grid voltage ( $V_G$ ), resulting in the situation shown in Figure 3. The comparison of these electronic characteristics with the herein observed shift of the pH titration curve allows the drawing of analogies. In our molecular version the triode produces an output in form of the **1MC** concentration, which is varied by pH and UV intensity, corresponding to  $i_A$ ,  $V_A$ , and  $V_G$ , respectively.

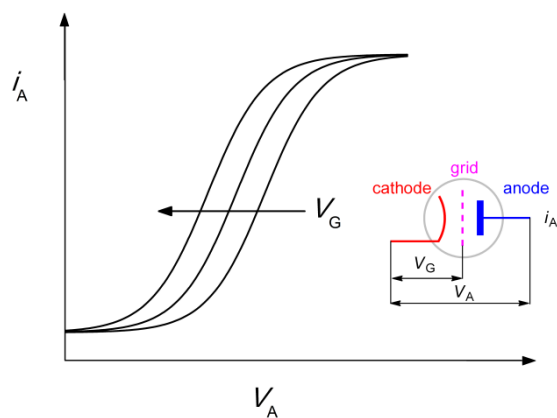


**Figure 3.** Characteristic  $i$ - $V$  curves of a triode on variation of the grid voltage ( $V_G$ ). The inset shows the electronic representation of a triode and the assignment of the applied potentials.

Based on the relevant rate and protonation constants the pH titration curve monitoring the concentration of **1MC** was modelled and showed virtually quantitative agreement with the experimental data (see ESI†). The discussed intricate interplay between the different forms of the network was further validated by monitoring the **1SP** and **1MCH** forms. Their observation is not directly linked to the readout of the absorbance at a specific wavelength as their absorption spectra overlap significantly. Therefore a system of equations that allows the numerical calculation of their concentrations was developed (see ESI†). Expectedly and in accordance with the corresponding modelling, monitoring the normalised concentration of **1MCH** revealed the opposite pH dependence than established for **1MC**, see ESI†. Finally, also the plot of the normalised concentration of **1SP** confirmed the applied lines of thought. Interestingly, but not unexpectedly, the titration curves for **1SP** are not shifted but inverted (Figure 4). In the absence of irradiation, the **SP** concentration is elevated at high pH (the **1SP/1MC** equilibrium is on the side of the ring-closed **SP** form; see above) and diminished at low pH (mostly due to the shifted equilibrium caused by the formation of the thermally stable **1MCH**). However, under irradiation this is inverted: the relative concentration of **1SP** is high at low pH (due to the efficient **1MCH**→**1SP** conversion) and low at high pH (due to the **1SP**→**1MC** conversion). Curiously, the application of attenuated UV intensity balances the network in such a way that virtually no pH dependence of the relative **1SP** concentration is observed.

In conclusion, the herein discovered photo-controlled shift of the pH titration curve, describing the acidochromic behaviour of the water-soluble spiropyran **1**, can be harnessed for the design of a molecular triode. The output of this device is read through the exclusive absorption signal of the **MC** form at 515 nm and the grid voltage is presented by the UV intensity. The described effects open the door to integrate the triode function with other features that can be introduced for example on the synthetically flexible indole nitrogen position.

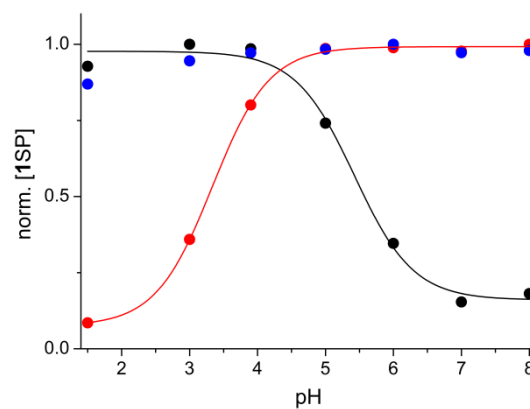


**Figure 4.** pH titration curves monitoring the normalised **1SP** concentration ( $[1SP]/[1SP]_{\max}$ ) in the dark (red), under full UV irradiation (254 nm; black) or attenuated UV irradiation (to 1.3% of full intensity; blue). The data were obtained under equilibrium conditions (i.e., thermal equilibrium and/or PSS). The sigmoid curves are meant to guide the eye.

Financial support from the Spanish *Ministerio de Economía y Competitividad* (grants CTQ2011-28390 and CTQ2014-54729-C2-1-P for U.P.), the *Junta de Andalucía* (P12-FQM-2140), FEDER, and the Swedish Research Council VR (grant 622-2010-280 for J.A.) is gratefully acknowledged.

## Notes and references

<sup>a</sup> Department of Chemistry and Chemical Engineering, Physical Chemistry, Chalmers University of Technology, SE-412 96 Gothenburg, Sweden.

<sup>b</sup> Department of Chemistry and Molecular Biology, University of Gothenburg, SE-412 96 Gothenburg, Sweden.

<sup>c</sup> CIQSO - Centre for Research in Sustainable Chemistry and Department of Chemistry, Campus El Carmen, University of Huelva, E-21071 Huelva, Spain.

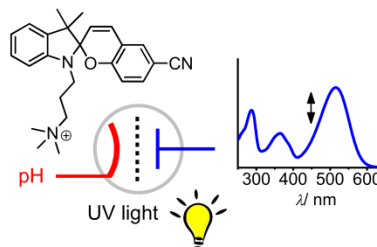
† Electronic Supplementary Information (ESI) available: additional experimental data, procedures for obtaining the concentrations of the different involved open and closed forms of **1** at each pH for the thermal and photochromic processes, modelling of the network. See DOI: 10.1039/c000000x/

‡ It was assumed that the isomerisation quantum yields are independent on the irradiation wavelength.

1. I. Yildiz, S. Impellizzeri, E. Deniz, B. McCaughan, J. F. Callan and F. M. Raymo, *J. Am. Chem. Soc.*, 2011, **133**, 871-879.
2. D. Gust, J. Andréasson, U. Pischel, T. A. Moore and A. L. Moore, *Chem. Commun.*, 2012, **48**, 1947-1957.
3. M. Natali and S. Giordani, *Chem. Soc. Rev.*, 2012, **41**, 4010-4029.
4. R. Tong, H. D. Hemmati, R. Langer and D. S. Kohane, *J. Am. Chem. Soc.*, 2012, **134**, 8848-8855.
5. A. P. de Silva, *Molecular Logic-based Computation*, The Royal Society of Chemistry, Cambridge, 2013.
6. J. J. Zhang, Q. Zou and H. Tian, *Adv. Mater.*, 2013, **25**, 378-399.
7. W. A. Velema, W. Szymanski and B. L. Feringa, *J. Am. Chem. Soc.*, 2014, **136**, 2178-2191.

8. R. Göstl, A. Senf and S. Hecht, *Chem. Soc. Rev.*, 2014, **43**, 1982-1996.
9. J. J. Zhang, J. X. Wang and H. Tian, *Mater. Horiz.*, 2014, **1**, 169-184.
10. G. de Ruiter and M. E. van der Boom, *J. Mater. Chem.*, 2011, **21**, 17575-17581.
11. M. Elstner, K. Weisshart, K. Müllen and A. Schiller, *J. Am. Chem. Soc.*, 2012, **134**, 8098-8100.
12. S. Erbas-Cakmak, O. A. Bozdemir, Y. Cakmak and E. U. Akkaya, *Chem. Sci.*, 2013, **4**, 858-862.
13. B. Rout, P. Milko, M. A. Iron, L. Motiei and D. Margulies, *J. Am. Chem. Soc.*, 2013, **135**, 15330-15333.
14. J. Andréasson and U. Pischel, *Chem. Soc. Rev.*, 2015, **44**, 1053-1069.
15. S. Silvi, E. C. Constable, C. E. Housecroft, J. E. Beves, E. L. Dunphy, M. Tomasulo, F. M. Raymo and A. Credi, *Chem. Eur. J.*, 2009, **15**, 178-185.
16. J. Kärrbratt, M. Hammarson, S. M. Li, H. L. Anderson, B. Albinsson and J. Andréasson, *Angew. Chem. Int. Ed.*, 2010, **49**, 1854-1857.
17. J. Andréasson, U. Pischel, S. D. Straight, T. A. Moore, A. L. Moore and D. Gust, *J. Am. Chem. Soc.*, 2011, **133**, 11641-11648.
18. P. Remón, M. Bälter, S. M. Li, J. Andréasson and U. Pischel, *J. Am. Chem. Soc.*, 2011, **133**, 20742-20745.
19. S. J. Chen, Y. H. Yang, Y. Wu, H. Tian and W. H. Zhu, *J. Mater. Chem.*, 2012, **22**, 5486-5494.
20. T. Avellini, H. Li, A. Coskun, G. Barin, A. Trabolsi, A. N. Basuray, S. K. Dey, A. Credi, S. Silvi, J. F. Stoddart and M. Venturi, *Angew. Chem. Int. Ed.*, 2012, **51**, 1611-1615.
21. M. Bälter, S. M. Li, J. R. Nilsson, J. Andréasson and U. Pischel, *J. Am. Chem. Soc.*, 2013, **135**, 10230-10233.
22. Y. Wu, Y. S. Xie, Q. Zhang, H. Tian, W. H. Zhu and A. D. Q. Li, *Angew. Chem. Int. Ed.*, 2014, **53**, 2090-2094.
23. A. E. Keirstead, J. W. Bridgewater, Y. Terazono, G. Kodis, S. Straight, P. A. Liddell, A. L. Moore, T. A. Moore and D. Gust, *J. Am. Chem. Soc.*, 2010, **132**, 6588-6595.
24. M. Pärss, C. C. Hofmann, K. Willinger, P. Bauer, M. Thelakkat and J. Köhler, *Angew. Chem. Int. Ed.*, 2011, **50**, 11405-11408.
25. A. J. M. Huxley, M. Schroeder, H. Q. N. Gunaratne and A. P. de Silva, *Angew. Chem. Int. Ed.*, 2014, **53**, 3622-3625.
26. I. Gallardo, G. Guirado, J. Hernando, S. Morais and G. Prats, *Chem. Sci.*, DOI: 10.1039/c5sc03395k.
27. J. Andersson, S. M. Li, P. Lincoln and J. Andréasson, *J. Am. Chem. Soc.*, 2008, **130**, 11836-11837.
28. M. Hammarson, J. Andersson, S. M. Li, P. Lincoln and J. Andréasson, *Chem. Commun.*, 2010, **46**, 7130-7132.
29. M. Hammarson, J. R. Nilsson, S. M. Li, P. Lincoln and J. Andréasson, *Chem. Eur. J.*, 2014, **20**, 15855-15862.
30. T. Sakata, Y. L. Yan and G. Marriott, *Proc. Nat. Acad. Sci. USA*, 2005, **102**, 4759-4764.
31. L. Y. Zhu, W. W. Wu, M.-Q. Zhu, J. J. Han, J. K. Hurst and A. D. Q. Li, *J. Am. Chem. Soc.*, 2007, **129**, 3524-3526.
32. G. Marriott, S. Mao, T. Sakata, J. Ran, D. K. Jackson, C. Petchprayoon, T. J. Gomez, E. Warp, O. Tulyathan, H. L. Aaron, E. Y. Isacoff and Y. L. Yan, *Proc. Nat. Acad. Sci. USA*, 2008, **105**, 17789-17794.
33. Z. Y. Tian, W. W. Wu, W. Wan and A. D. Q. Li, *J. Am. Chem. Soc.*, 2009, **131**, 4245-4252.
34. N. Shao, J. Y. Jin, S. M. Cheung, R. H. Yang, W. H. Chan and T. Mo, *Angew. Chem. Int. Ed.*, 2006, **45**, 4944-4948.
35. Y. Hirshberg, *J. Am. Chem. Soc.*, 1956, **78**, 2304-2312.
36. G. Berkovic, V. Krongauz and V. Weiss, *Chem. Rev.*, 2000, **100**, 1741-1754.
37. F. M. Raymo and S. Giordani, *J. Am. Chem. Soc.*, 2001, **123**, 4651-4652.
38. F. M. Raymo and S. Giordani, *Proc. Nat. Acad. Sci. USA*, 2002, **99**, 4941-4944.
39. P. L. Gentili, A. L. Rightler, B. M. Heron and C. D. Gabbutt, *Chem. Commun.*, 2016, **52**, 1474-1477.
40. M. Hammarson, J. R. Nilsson, S. M. Li, T. Beke-Somfai and J. Andréasson, *J. Phys. Chem. B*, 2013, **117**, 13561-13571.
41. T. Stafforst and D. Hilvert, *Chem. Commun.*, 2009, 287-288.
42. M. V. Peters, R. S. Stoll, A. Kühn and S. Hecht, *Angew. Chem. Int. Ed.*, 2008, **47**, 5968-5972.
43. S. Samanta, A. Babalhavaeji, M.-X. Dong and G. A. Woolley, *Angew. Chem. Int. Ed.*, 2013, **52**, 14127-14130.

#### TOC graph



A molecular triode that is operated by pH and light can be implemented with spiropyrans.